

# An internuclear J-coupling of $^3\text{He}$ induced by molecular confinement

George Razvan Bacanu, Jyrki Rantaharju, Gabriela Hoffman, Mark C. Walkey, Sally Bloodworth, Maria Concistrè, Richard J. Whitby, and Malcolm H. Levitt\*

*Department of Chemistry, University of Southampton, SO17 1BJ, UK*

E-mail: mhl@soton.ac.uk

Phone: +44 (0)23 80596753

## Abstract

The solution-state  $^{13}\text{C}$  NMR spectrum of the endofullerene  $^3\text{He}@C_{60}$  displays a doublet structure due to a J-coupling of magnitude  $77.5 \pm 0.2$  mHz at 340 K between the  $^3\text{He}$  nucleus and a  $^{13}\text{C}$  nucleus of the enclosing carbon surface. The J-coupling increases in magnitude with increasing temperature. Quantum chemistry calculations successfully predict the approximate magnitude of the coupling. This observation shows that the mutual proximity of molecular or atomic species is sufficient to induce a finite scalar nuclear spin-spin coupling, providing that translational motion is restricted by confinement. The phenomenon may have applications to the study of surface interactions and to mechanically bound species.

The indirect nuclear spin-spin coupling (J-coupling) is one of the most useful interactions in high-resolution nuclear magnetic resonance (NMR). It often leads to characteristic multiplet splittings in high-resolution NMR spectra which are invaluable for the determination of molecular structure.<sup>1</sup>

The dependence of the three-bond J-coupling on molecular torsional angles makes it particularly useful for the determination of molecular conformations in chemistry and structural biol-

ogy.<sup>2,3</sup> J-couplings are also transmitted through hydrogen bonds.<sup>4-7</sup> There is also indirect experimental evidence from noble gas magnetometry, supported by computational studies, for very small internuclear J-couplings between species associated by van der Waals forces.<sup>8-10</sup>

Although the J-coupling is often regarded as a signature of chemical bonding, it has long been known that J-couplings may also be induced by the overlap of electron clouds forced by steric constraints – especially when electron lone pairs are involved. Such interactions are often referred to as “through-space” or “non-bonded” J-couplings.<sup>11-13</sup> Although this nomenclature is contentious, these interactions are useful for the elucidation of molecular structure and conformation in systems of constrained molecular geometry.<sup>12,14</sup> Quantum chemistry has been used to estimate such couplings.<sup>10,15-19</sup>

In principle, the mere confinement of atoms and molecules to the same region of space may induce an internuclear J-coupling through the overlap of electron clouds. However, to our knowledge, the only experimental evidence for such “confinement-induced” J-couplings comes from double-quantum NMR data on  $^{129}\text{Xe}$  in microporous solids,<sup>20</sup> which have been interpreted in terms of anisotropic  $^{129}\text{Xe}$ - $^{129}\text{Xe}$  J-couplings, supported by quantum chemistry calculations.<sup>19</sup>

We now provide direct spectroscopic evidence for a “confinement-induced” J-coupling

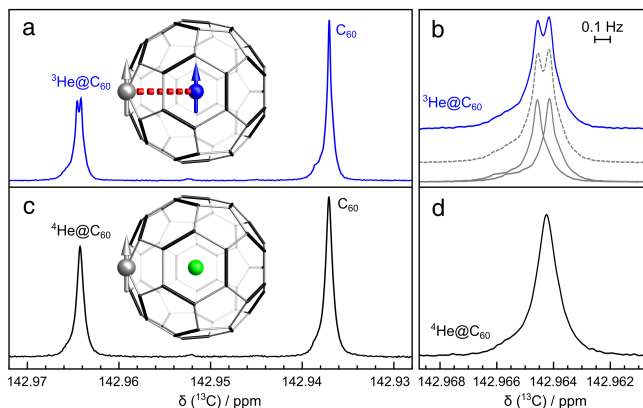


Figure 1: **(a)**  $^{13}\text{C}$  solution NMR spectra of a  $\sim 25$  mM solution of  $^3\text{He}@C_{60}$  (43% filling factor) in ODCB- $d_4$  at 340 K and 16.45 T, using a Bruker AVANCE NEO console and a TCI prodigy 5mm cryoprobe (average of 40 transients); **(b)** Blue line: expansion of the  $^{13}\text{C}$  peak of  $^3\text{He}@C_{60}$ ; Dashed grey line: Best fit to two shifted spectral components, each with a shape matching the  $^{13}\text{C}$  peak of  $C_{60}$ ; Solid gray lines: individual spectral components. **(c)**  $^{13}\text{C}$  solution NMR spectra of a  $\sim 25$  mM solution of  $^4\text{He}@C_{60}$  (41% filling factor) in ODCB- $d_4$  (average of 32 transients). All other conditions are the same as in **(a)**. **(d)** Expansion of the  $^{13}\text{C}$  peak of  $^4\text{He}@C_{60}$ .

between  $^3\text{He}$  and  $^{13}\text{C}$  nuclei in the noble gas endofullerene  $^3\text{He}@C_{60}$ . The  $^3\text{He}$  nucleus has spin  $I = 1/2$  and a relatively large gyromagnetic ratio (approximately 3–4 of that of the proton). The spin-lattice relaxation times  $T_1$  of  $^3\text{He}$  and  $^{13}\text{C}$  are both long (many tens of seconds) in solution, providing high intrinsic spectral resolution (see Supporting Information).

Noble gas endofullerenes are available in significant quantities through the “molecular surgery” synthetic route.<sup>21,22</sup> Samples of  $^3\text{He}@C_{60}$  and  $^4\text{He}@C_{60}$  were prepared by an analogous procedure to that described in reference 23. The  $^{13}\text{C}$  NMR spectrum of a  $\sim 25$  mM solution of  $^3\text{He}@C_{60}$  (filling factor  $f = 0.43$ ) in *ortho*-dichlorobenzene- $d_4$  (ODCB- $d_4$ ) at 340 K is shown in Fig. 1(a,b). The spectrum shows  $^{13}\text{C}$  peaks from both empty  $C_{60}$  and  $^3\text{He}@C_{60}$ . There is a shift of 0.027 ppm between the  $^{13}\text{C}$  peaks of  $^3\text{He}@C_{60}$  and  $C_{60}$ , consistent with previous measurements.<sup>21</sup> A small splitting of the

$^{13}\text{C}$  peak of  $^3\text{He}@C_{60}$  is clearly visible. The splitting is also present on the pair of small  $^{13}\text{C}$  “side peaks” of  $^3\text{He}@C_{60}$ , which are due to  $^{13}\text{C}_2$  isotopomers<sup>24</sup> (see Supporting Information). The splitting is absent in the  $^{13}\text{C}$  peak of empty  $C_{60}$ , and is also absent in the spectrum of  $^4\text{He}@C_{60}$ , which is shown in Fig. 1(c,d). The  $^{13}\text{C}$  chemical shifts of  $^4\text{He}@C_{60}$  and  $^3\text{He}@C_{60}$  are within 0.2 ppb of each other.

The sharp  $^{13}\text{C}$  peak of  $C_{60}$  in figure 1(a) has a linewidth-at-half-height of 96 mHz, with small shoulders due to residual field inhomogeneity. To estimate the splitting, the unsplit  $^{13}\text{C}$  peak of empty  $C_{60}$  was first interpolated by a spline function, and two such functions superposed to fit the doublet structure as illustrated in Fig. 1b by the gray lines. This leads to the following estimate of the doublet splitting:  $77.5 \pm 0.2$  mHz at 340 K. An identical estimate of the splitting was obtained by reference deconvolution.<sup>25</sup>

We attribute the splitting in the  $^{13}\text{C}$  spectrum of  $^3\text{He}@C_{60}$  to a “non-bonded” or “through-space”  $^0J_{\text{HeC}}$  coupling between the  $l = 1/2$  nuclear spin of  $^3\text{He}$  and that of a  $^{13}\text{C}$  nucleus in the cage (also  $l = 1/2$ ). The absence of a splitting for  $^4\text{He}@C_{60}$  is consistent with the zero nuclear spin of the  $^4\text{He}$  isotope. The “0” prefix in the notation  $^0J_{\text{HeC}}$  indicates the absence of a formal chemical bond between the two atoms. After accounting for the gyromagnetic ratios, this value is roughly consistent with the reported values for “non-bonded” J-couplings in proteins.<sup>14</sup>

This is, to our knowledge, the first direct spectroscopic observation of a J-coupling involving the  $^3\text{He}$  nucleus. The sign of  $^0J_{\text{HeC}}$  has not yet been determined experimentally, although there is computational evidence that it is negative (see below). Experiments are planned in which cross-correlated relaxation effects are used to determine its sign.<sup>26</sup>

The magnitude of the  $^0J_{\text{HeC}}$  coupling increases slightly with increasing temperature, as shown in Figure 2. The splitting has an approximately linear dependence on  $T$  over the plotted temperature range, following the equation  $|^0J_{\text{HeC}}| = mT + c$ , where the intercept is  $c = 51.4 \pm 0.7$  mHz, and the slope is  $m = (76.7 \pm 2.3) \times 10^{-3}$  mHz K<sup>-1</sup>.

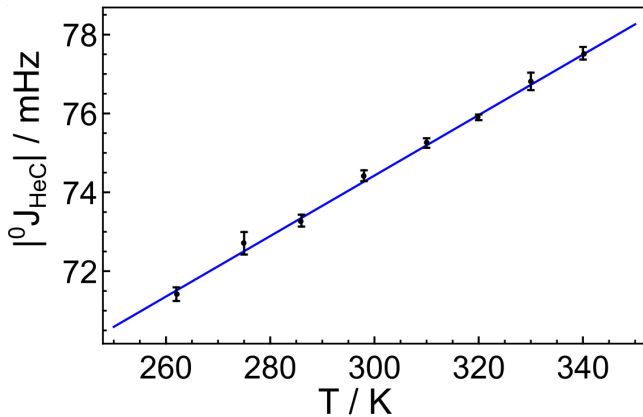


Figure 2: Temperature dependence of the  ${}^3\text{He}$ - ${}^{13}\text{C}$  spin-spin coupling  ${}^0J_{\text{HeC}}$ , for a  $\sim 25$  mM solution of  ${}^3\text{He}@C_{60}$  (filling factor  $f = 0.43$ ) in *ortho*-dichlorobenzene- $d_4$ . The solid blue line shows the best linear fit,  $|{}^0J_{\text{HeC}}| = mT + c$ , with  $c = 51.4$  mHz and  $m = 76.7 \times 10^{-3}$  mHz K $^{-1}$ .

The  ${}^0J_{\text{HeC}}$  coupling was estimated by quantum chemistry techniques.<sup>27</sup> Computational details are given in the Supporting Information. In common with related work,<sup>10,15–17,19</sup> the calculation of  ${}^0J_{\text{HeC}}$  treated the  ${}^{13}\text{C}$  and  ${}^3\text{He}$  nuclei as localised points, ignoring the quantum delocalization of the nuclear wavefunctions.

Since *ab initio* calculations of the complete  ${}^3\text{He}@C_{60}$  system are computationally very demanding, we first performed test computations on the much simpler system of a  ${}^3\text{He}$  atom located on the six-fold symmetry axis of a  $C_6H_6$  molecule.<sup>28</sup> Independent computations were performed for a variety of He positions along the six-fold symmetry axis. In each case, the J-coupling constant between a  ${}^{13}\text{C}$  nucleus on the benzene ring and the  ${}^3\text{He}$  nucleus was calculated using CC theory at the CCSD level, using the ccJ-pVDZ basis.<sup>29</sup>

The results on the  ${}^3\text{He} \dots C_6H_6$  model system are shown as a function of the  ${}^{13}\text{C} \dots {}^3\text{He}$  distance by the green circles in figure 3. The J-coupling is predicted to be negative, with a magnitude decreasing as the  ${}^3\text{He} \dots {}^{13}\text{C}$  distance increases, consistent with the decreasing overlap of the electron clouds of the interacting species.

The CCSD calculations on the  ${}^3\text{He} \dots C_6H_6$  model system were used to benchmark DFT-functionals with the pcJ-X (X=0-4) basis sets<sup>30</sup>

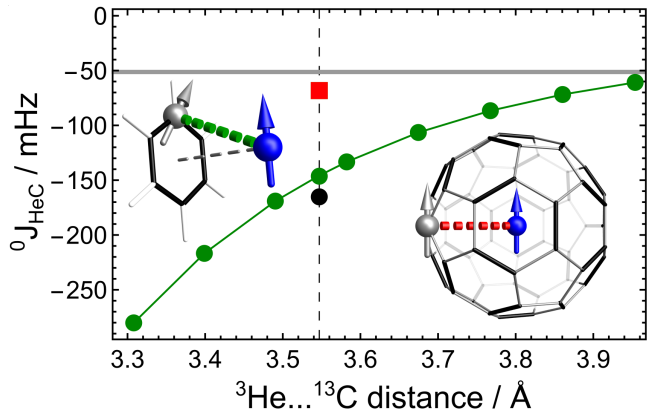


Figure 3:  ${}^3\text{He}$ - ${}^{13}\text{C}$  J-couplings calculated by quantum chemistry techniques. Green circles: Results of the *ab initio* CCSD calculations on the  ${}^3\text{He} \dots C_6H_6$  model system. The solid green line is a guide for the eye. Black circle: DFT benchmark calculation of the  ${}^3\text{He} \dots C_6H_6$  model system. Red square: DFT-calculated J-coupling of the  ${}^3\text{He}@C_{60}$  endofullerene. The horizontal gray band shows the confidence limits of the zero-Kelvin intercept of the linear temperature-dependence of  $|{}^0J_{\text{HeC}}|$ , as shown in figure 2. The vertical dashed line shows the internuclear distance of  $3.547 \text{ \AA}$  between the  ${}^3\text{He}$  and  ${}^{13}\text{C}$  nuclei in  ${}^3\text{He}@C_{60}$ .

(details in the Supporting Information). The DFT calculations converged to a good approximation to the CCSD result when using the PBE0 functional with 75% of exact exchange.<sup>31,32</sup> The result of the optimised DFT calculation on the  ${}^3\text{He} \dots C_6H_6$  system is shown by the black circle in Fig. 3.

A DFT calculation of  ${}^0J_{\text{HeC}}$  for the complete  ${}^3\text{He}@C_{60}$  system was performed using the benchmarked functional and the pcJ-3 basis. The position of the He atom was within  $0.01 \text{ \AA}$  of the cage centre in the optimized structure. The estimated J-coupling is  $-68.3$  mHz, as shown by the red square in Fig. 3. The contributions of the different terms are discussed in the Supporting Information. The result is in reasonable agreement with the extrapolation of the experimental temperature-dependent J-splitting down to zero Kelvin, which gives an estimate of  $|{}^0J_{\text{HeC}}|(0 \text{ K}) \simeq 51.4$  mHz (see figure 2).

The increase of the J-coupling with increasing

temperature may be understood qualitatively using either classical or quantum reasoning. In the classical argument, an increase in temperature causes increased average kinetic energy for the He atom, and hence increased penetration of the He atom into the carbon electron clouds upon collisions with the wall.<sup>33</sup> The increased overlap of the He and C electron clouds leads in turn to an increase in the  ${}^0J_{\text{HeC}}$  coupling magnitude upon an increase in temperature. The corresponding quantum reasoning involves the quantum wavefunction of the encapsulated atom. The “particle-in-a-box” quantization of the guest species in endofullerenes has been investigated extensively for similar systems.<sup>34–37</sup> In these cases, the ground-state quantum translational wavefunction is strongly localised in the centre of the box. An increase in temperature populates excited quantum states, which have larger probability amplitude at large displacement from the cage centre, i.e. close to the walls of the box. Hence this argument also predicts a closer approach of the He and C nuclei on average when the temperature is increased, leading to an increase in the  ${}^0J_{\text{HeC}}$  coupling magnitude with increasing temperature.

This is not the first time an attempt was made to resolve a J-coupling between the nucleus of a noble gas atom and a fullerene  ${}^{13}\text{C}$  nucleus. Previous NMR measurements of  ${}^{129}\text{Xe}@C_{60}$  failed to resolve a J-coupling, possibly due to the small sample amount and limited spectral resolution.<sup>38</sup>

In summary we have obtained direct experimental evidence for a scalar spin-spin coupling between a  ${}^3\text{He}$  nucleus and the  ${}^{13}\text{C}$  nucleus of a carbon surface. The coupling is made visible by the confinement of the noble gas atom to the close proximity of the surface sites by the encapsulating fullerene cage. To our knowledge, this is the first direct observation of a J-coupling involving the  ${}^3\text{He}$  nucleus. Furthermore, the observation indicates that the nuclei of any pair of molecules or atoms which are confined in close proximity may display an internuclear J-coupling. J-couplings across molecular surfaces may be useful for the study of mechanically interlocked molecules,<sup>39</sup> and may allow the efficient transfer of hyper-

polarization from optically-pumped noble gases to biomolecules, as in biosensor applications.<sup>40</sup> Further work is under way to estimate the sign and accurate magnitude of the  ${}^0J_{\text{HeC}}$  coupling using double-resonance techniques, and to detect similar internuclear couplings in other spatially confined systems, such as molecular endofullerenes.<sup>37,41–43</sup>

**Acknowledgement** This research was supported by EPSRC (UK), grant codes EP/P009980/1, EP/P030491/1, EP/K00509X/1 and EP/T004320/1, the European Research Council (786707-FunMagResBeacons), the Marie Skłodowska-Curie grant 891400 of the European Union, and the IRIDIS High Performance Computing Facility at the University of Southampton. We thank Dr Neil Wells for experimental help.

## Supporting Information Available

Computational details, NMR relaxation curves, and NMR spectra of the helium endofullerenes, showing the  ${}^0J_{\text{HeC}}$  splitting of the  ${}^{13}\text{C}_2$  side peaks.

## References

- (1) Corio, P. L. *Structure of High-Resolution NMR Spectra*; Academic Press: New York, 1966.
- (2) Karplus, M. Vicinal Proton Coupling in Nuclear Magnetic Resonance. *J. Am. Chem. Soc.* **1963**, *85*, 2870–2871.
- (3) Cavanagh, J.; Fairbrother, W. J.; Palmer III, A. G.; Rance, M.; Skelton, N. J. *Protein NMR Spectroscopy. Principles and Practice*, 2nd ed.; Elsevier Academic Press: Amsterdam, 2007.
- (4) Dingley, A. J.; Grzesiek, S. Direct Observation of Hydrogen Bonds in Nucleic Acid Base Pairs by Internucleotide 2JNN Couplings. *Journal of the American Chemical Society* **1998**, *120*, 8293–8297.

- (5) Pervushin, K.; Ono, A.; Fernández, C.; Szyperski, T.; Kainosho, M.; Wüthrich, K. NMR Scalar Couplings across Watson–Crick Base Pair Hydrogen Bonds in DNA Observed by Transverse Relaxation-Optimized Spectroscopy. *PNAS* **1998**, *95*, 14147–14151.
- (6) Cordier, F.; Grzesiek, S. Direct Observation of Hydrogen Bonds in Proteins by Interresidue  $^3\text{hJNC}'$  Scalar Couplings. *J. Am. Chem. Soc.* **1999**, *121*, 1601–1602.
- (7) Brown, S. P.; Perez-Torralba, M.; Sanz, D.; Claramunt, R. M.; Emsley, L. The Direct Detection of a Hydrogen Bond in the Solid State by NMR through the Observation of a Hydrogen-Bond Mediated  $\text{N}15\text{-N}15$  J Coupling. *J. Am. Chem. Soc.* **2002**, *124*, 1152–1153.
- (8) Ledbetter, M. P.; Saielli, G.; Bagno, A.; Tran, N.; Romalis, M. V. Observation of Scalar Nuclear Spin–Spin Coupling in van Der Waals Complexes. *PNAS* **2012**, *109*, 12393–12397.
- (9) Limes, M. E.; Dural, N.; Romalis, M. V.; Foley, E. L.; Kornack, T. W.; Nelson, A.; Grisham, L. R.; Vaara, J. Dipolar and Scalar  $^3\text{He}\text{-}^{129}\text{Xe}$  Frequency Shifts in Stemless Cells. *Phys. Rev. A* **2019**, *100*, 010501.
- (10) Vaara, J.; Romalis, M. V. Calculation of Scalar Nuclear Spin-Spin Coupling in a Noble-Gas Mixture. *Phys. Rev. A* **2019**, *99*, 060501.
- (11) Davis, D. R.; Lutz, R. P.; Roberts, J. D. Nuclear Magnetic Resonance Spectroscopy. Long-Range Spin-Spin Couplings In Saturated Molecules. *J. Am. Chem. Soc.* **1961**, *83*, 246–247.
- (12) Hierso, J.-C. Indirect Nonbonded Nuclear Spin–Spin Coupling: A Guide for the Recognition and Understanding of “Through-Space” NMR J Constants in Small Organic, Organometallic, and Coordination Compounds. *Chem. Rev.* **2014**, *114*, 4838–4867.
- (13) Griffin, J. M.; Yates, J. R.; Berry, A. J.; Wimperis, S.; Ashbrook, S. E. High-Resolution  $^{19}\text{F}$  MAS NMR Spectroscopy: Structural Disorder and Unusual J Couplings in a Fluorinated Hydroxy-Silicate. *Journal of the American Chemical Society* **2010**, *132*, 15651–15660.
- (14) Plevin, M. J.; Bryce, D. L.; Boisbouvier, J. Direct Detection of  $\text{CH}/\text{O}$  Interactions in Proteins. *Nature Chemistry* **2010**, *2*, 466–471.
- (15) Salsbury Jr., F. R.; Harris, R. A. Estimation of the Fermi Contact Contribution to the Xenon-Hydrogen and Xenon-Xenon Spin-Spin Coupling Constants. *Molecular Physics* **1998**, *94*, 307–312.
- (16) Pecul, M. The Nuclear Spin–Spin Coupling Constant in  $\text{He}_2$ . *J. Chem. Phys.* **2000**, *113*, 10835–10836.
- (17) Bryce, D. L.; Wasylishen, R. E. Ab Initio Characterization of Through-Space Indirect Nuclear Spin–Spin Coupling Tensors for Fluorine-X ( $\text{X}=\text{F}, \text{C}, \text{H}$ ) Spin Pairs. *Journal of Molecular Structure* **2002**, *602-603*, 463–472.
- (18) Vaara, J.; Hanni, M.; Jokisaari, J. Nuclear Spin-Spin Coupling in a van Der Waals-Bonded System: Xenon Dimer. *J. Chem. Phys.* **2013**, *138*, 104313.
- (19) Jokisaari, J.; Vaara, J. Nuclear Spin–Spin Coupling Anisotropy in the van Der Waals-Bonded  $^{129}\text{Xe}$  Dimer. *Phys. Chem. Chem. Phys.* **2013**, *15*, 11427–11430.
- (20) Brouwer, D. H.; Alavi, S.; Ripmeester, J. A. A Double Quantum  $^{129}\text{Xe}$  NMR Experiment for Probing Xenon in Multiply-Occupied Cavities of Solid-State Inclusion Compounds. *Phys. Chem. Chem. Phys.* **2007**, *9*, 1093–1098.
- (21) Morinaka, Y.; Tanabe, F.; Murata, M.; Murata, Y.; Komatsu, K. Rational Synthesis, Enrichment, and  $^{13}\text{C}$  NMR Spectra of Endohedral  $\text{C}_{60}$  and  $\text{C}_{70}$  Encapsu-

- lating a Helium Atom. *Chem. Commun.* **2010**, *46*, 4532–4534.
- (22) Bloodworth, S.; Hoffman, G.; Walkey, M. C.; Bacanu, G. R.; Herniman, J.; Levitt, M. H.; Whitby, R. J. Synthesis of Ar@C60 Using Molecular Surgery. *Chem. Commun.* **2020**, *56*, 10521–10524.
- (23) Krachmalnicoff, A.; Levitt, M. H.; Whitby, R. J. An Optimised Scalable Synthesis of H2O@C60 and a New Synthesis of H2@C60. *Chem. Commun.* **2014**, *50*, 13037–13040.
- (24) Bacanu, G. R.; Hoffman, G.; Ampon-sah, M.; Concistrè, M.; Whitby, R. J.; Levitt, M. H. Fine Structure in the Solution State <sup>13</sup>C-NMR Spectrum of C60 and Its Endofullerene Derivatives. *Physical Chemistry Chemical Physics* **2020**, *22*, 11850–11860.
- (25) Morris, G. A.; Barjat, H.; Home, T. J. Reference Deconvolution Methods. *Progress in Nuclear Magnetic Resonance Spectroscopy* **1997**, *31*, 197–257.
- (26) Goldman, M. Interference Effects in the Relaxation of a Pair of Unlike Spin-1/2 Nuclei. *Journal of Magnetic Resonance (1969)* **1984**, *60*, 437–452.
- (27) Jensen, F. *Introduction to Computational Chemistry*, 3rd ed.; Wiley, Chichester, 2017.
- (28) Straka, M.; Lantto, P.; Vaara, J. Toward Calculations of the <sup>129</sup>Xe Chemical Shift in Xe@C60 at Experimental Conditions: Relativity, Correlation, and Dynamics. *J. Phys. Chem. A* **2008**, *112*, 2658–2668.
- (29) Benedikt, U.; Auer, A. A.; Jensen, F. Optimization of Augmentation Functions for Correlated Calculations of Spin-Spin Coupling Constants and Related Properties. *J. Chem. Phys.* **2008**, *129*, 064111.
- (30) Jensen, F. The Basis Set Convergence of Spin-Spin Coupling Constants Calculated by Density Functional Methods. *J. Chem. Theory Comput.* **2006**, *2*, 1360–1369.
- (31) Adamo, C.; Barone, V. Toward Chemical Accuracy in the Computation of NMR Shieldings: The PBE0 Model. *Chemical Physics Letters* **1998**, *298*, 113–119.
- (32) Adamo, C.; Barone, V. Toward Reliable Density Functional Methods without Adjustable Parameters: The PBE0 Model. *J. Chem. Phys.* **1999**, *110*, 6158–6170.
- (33) Even, W.; Smith, J.; Roth, M. W. Molecular Dynamics Simulations of Noble Gases Encapsulated in C60 Fullerene. *Molecular Simulation* **2005**, *31*, 207–213.
- (34) Mamone, S.; Ge, M.; Huvonen, D.; Nagel, U.; Danquigny, A.; Cuda, F.; Grossel, M. C.; Murata, Y.; Komatsu, K.; Levitt, M. H.; Rõõm, T.; Carravetta, M. Rotor in a Cage: Infrared Spectroscopy of an Endohedral Hydrogen-Fullerene Complex. *J. Chem. Phys.* **2009**, *130*, 081103–4.
- (35) Horsewill, A. J.; Rols, S.; Johnson, M. R.; Murata, Y.; Murata, M.; Komatsu, K.; Carravetta, M.; Mamone, S.; Levitt, M. H.; Chen, J. Y. C.; Johnson, J. A.; Lei, X.; Turro, N. J. Inelastic Neutron Scattering of a Quantum Translator-Rotator Encapsulated in a Closed Fullerene Cage: Isotope Effects and Translation-Rotation Coupling in H<sub>2</sub>@C<sub>60</sub> and HD@C<sub>60</sub>. *Physical Review B* **2010**, *82*, 081410.
- (36) Beduz, C.; Carravetta, M.; Chen, J. Y.-C.; Concistrè, M.; Denning, M.; Frunzi, M.; Horsewill, A. J.; Johannessen, O. G.; Lawler, R.; Lei, X.; Levitt, M. H.; Li, Y.; Mamone, S.; Murata, Y.; Nagel, U.; Nishida, T.; Olivier, J.; Rols, S.; Rõõm, T.; Sarkar, R.; Turro, N. J.; Yang, Y. Quantum Rotation of Ortho and Para-Water Encapsulated in a Fullerene Cage. *Proceedings of the National Academy of Sciences* **2012**, *109*, 12894–12898.

- (37) Krachmalnicoff, A.; Bounds, R.; Mamone, S.; Alom, S.; Concistrè, M.; Meier, B.; Kouřil, K.; Light, M. E.; Johnson, M. R.; Rols, S.; Horsewill, A. J.; Shugai, A.; Nagel, U.; Rõõm, T.; Caravetta, M.; Levitt, M. H.; Whitby, R. J. The Dipolar Endofullerene HF@C60. *Nat Chem* **2016**, *8*, 953–957.
- (38) Syamala, M. S.; Cross, R. J.; Saunders, M. 129Xe NMR Spectrum of Xenon Inside C60. *J. Am. Chem. Soc.* **2002**, *124*, 6216–6219.
- (39) Stoddart, J. F. The Chemistry of the Mechanical Bond. *Chem. Soc. Rev.* **2009**, *38*, 1802–1820.
- (40) Schröder, L.; Lowery, T. J.; Hilty, C.; Wemmer, D. E.; Pines, A. Molecular Imaging Using a Targeted Magnetic Resonance Hyperpolarized Biosensor. *Science* **2006**, *314*, 446–449.
- (41) Komatsu, K.; Murata, M.; Murata, Y. Encapsulation of Molecular Hydrogen in Fullerene C60 by Organic Synthesis. *Science* **2005**, *307*, 238–240.
- (42) Kurotobi, K.; Murata, Y. A Single Molecule of Water Encapsulated in Fullerene C60. *Science* **2011**, *333*, 613–616.
- (43) Bloodworth, S.; Sitinova, G.; Alom, S.; Vidal, S.; Bacanu, G. R.; Elliott, S. J.; Light, M. E.; Herniman, J. M.; Langley, G. J.; Levitt, M. H.; Whitby, R. J. First Synthesis and Characterization of CH4@C60. *Angewandte Chemie International Edition* **2019**, *58*, 5038–5043.

